

Analyst

Accepted Manuscript



This is an *Accepted Manuscript*, which has been through the Royal Society of Chemistry peer review process and has been accepted for publication.

Accepted Manuscripts are published online shortly after acceptance, before technical editing, formatting and proof reading. Using this free service, authors can make their results available to the community, in citable form, before we publish the edited article. We will replace this *Accepted Manuscript* with the edited and formatted *Advance Article* as soon as it is available.

You can find more information about *Accepted Manuscripts* in the [Information for Authors](#).

Please note that technical editing may introduce minor changes to the text and/or graphics, which may alter content. The journal's standard [Terms & Conditions](#) and the [Ethical guidelines](#) still apply. In no event shall the Royal Society of Chemistry be held responsible for any errors or omissions in this *Accepted Manuscript* or any consequences arising from the use of any information it contains.



Journal Name

ARTICLE

Analysis of cobalt phosphide (CoP) nanorods designed for non-enzyme glucose detection

Received 00th January 20xx,
Accepted 00th January 20xx

DOI: 10.1039/x0xx00000x

www.rsc.org/

Qiang-Qiang Sun, Min Wang*, Shu-Juan Bao*, Yu Chen Wang, Shuang Gu

Nanorods of cobalt phosphide have been prepared and evaluated as an electrocatalyst for non-enzyme glucose detection. The nanorods were used to modify the surface of an electrode and detect glucose without the help of an enzyme for the first time. The crystal structure and composition of cobalt phosphide were identified by XRD and XPS, respectively, and the morphology of the as-prepared samples was observed by FESEM and TEM. The electrochemical measurement results indicate that the CoP-based sensor exhibits excellent catalytic activity and a far lower detection potential compared to that of bare GCE. Specifically, the electrocatalytic mechanism of CoP in the detection of glucose was proposed based on a series of physical characterizations, electrochemical measurements, and theoretical calculation.

Introduction

Developing a fast and reliable method for glucose determination is immensely important in many fields, including clinical diagnostics, the food industry, and in the preparation of biological and chemical samples. Throughout the past decades, a great deal of effort has been devoted to exploring reliable glucose sensing techniques, such as fluorescent¹, optical², electro-chemiluminescence³, surface plasmon resonance⁴, and electrochemical methods.⁵ Among these techniques, the electrochemical method has become the most highly desirable for sensor research. Electrochemical methods can be classified into glucose oxidase-based sensing and non-enzymatic glucose sensing. Glucose oxidase is a type of bio-enzyme that possesses high sensitivity and selectivity to glucose and has been widely used to construct various amperometric biosensors for glucose detection. However, due to the intrinsic properties of the enzyme, glucose oxidase-based biosensors suffer from instability. Therefore, it is of great importance to develop sensitive and selective non-enzymatic sensors for glucose detection. The enzymeless detection of glucose by conventional electrochemical methods is not just of recent interest; continued efforts have been made since early studies.⁶⁻⁸ However, the electrocatalytic oxidation process of glucose on bare platinum or a carbon surface illustrates that the overall kinetics of glucose oxidation is too slow to produce a significant faradaic current, which is important for collecting the signal of glucose. Hence, searching for excellent catalyst materials to reduce the activation energy and to understand the mechanisms of electrocatalytic glucose is very important for designing a good enzyme-free glucose

sensor. With the development of nanoscience and nanotechnology, an increasing amount of nanomaterials, including various metals (e.g., Au, Pd, Pt, and Cu⁹⁻¹²) and transition metal oxides (e.g., CuO, NiO, Co₃O₄, MnO₂, etc.¹³⁻¹⁶) have been used to modify the enzyme-free biosensor electrodes. While such research has boosted the development of enzyme-free bioelectroanalysis, studies on the mechanism still require further investigation.

Cobalt phosphides have recently received increasing attention due to their catalytic and magnetic properties as well as their potential as a promising electrode material.¹⁷⁻¹⁹ The valence of Co is changeable, and Co can be easily exposed in the orthorhombic crystal of CoP; thus, CoP can be used in catalytic oxidation to reduce substances like glucose. However, to the best of our knowledge, the use of CoP for enzyme-free bioelectroanalysis of glucose remains unexplored.

In this featured work, we present the fundamental study of CoP nanorods used in glucose sensing. The designed biosensor should exhibit a typical amperometric response in an alkaline solution without the help of an enzyme; this behavior satisfies the requirements for an electrocatalytic material of a glucose biosensor. Furthermore, the mechanism of glucose oxidation on CoP surface is discussed in detail, which is meaningful for searching for excellent catalyst materials for an enzyme-free glucose sensor.

Experiment

Reagents

Cobalt nitrate (Co(NO₃)₂·6H₂O), urea (CO(NH₂)₂) and Nafion were purchased from Sigma-Aldrich. Sodium hypophosphite (NaH₂PO₂) was purchased from Aladdin Industrial. All chemical reagents used as received without further purification.

*Institute for Clean Energy & Advanced Materials, Faculty of Materials and Energy, Southwest University, Chongqing, 400715, P. R. China.
E-mail: minwang@swu.edu.cn; baoshj@swu.edu.cn.*

Synthesis of material

In 80 mL of deionized water, 2.3 g of $\text{Co}(\text{NO}_3)_2 \cdot 6\text{H}_2\text{O}$ and 2.4 g of urea were added to form a pink solution under stirring. The solution was kept at 90°C for 12 h to produce a precipitate, which was considered as the precursor for next reaction. The as-obtained precipitate was filtered and washed with deionized water. Successively, the precursor was dried at 60°C for 10 h. Finally, cobalt phosphide was fabricated by low-temperature phosphidation of the obtained Co-based precursor as following: annealing 0.2 g of as-prepared precursor in a tubular furnace at 350°C for 1.5 h with 2.5 g of NaH_2PO_2 in Ar flow. Noticeably, NaH_2PO_2 was placed in front of the precursor separately in the Ar flow direction.

Characterization of the materials

The morphologies of precursor and final product were characterized by field emission scanning electron microscope (FESEM, JSM-7800F, Japan) and transmission electron microscope (TEM, JEM-2100, Japan). Their crystal structure was determined by powder X-ray diffraction (XRD, XRD-7000). The X-ray photoelectron spectroscopy (XPS) data were obtained by a spectrometer (Escalab 250xi, Thermo Scientific).

Electrochemical measurement

CoP was dispersed in deionized water to form 10 mg/ml CoP suspension. Glass carbon electrode (GCE) with a diameter of 3 mm was polished with 0.3 and 0.05 μm alumina powder, followed by rinsing with deionised water. Then the electrode was dried at room temperature. Next, 5 μL of the above suspension was dropped on the center of GCE and dried naturally. Finally, 10 μL of 0.5 wt% Nafion solution was placed on the whole plate of GCEs to form Nafion membrane. The as-fabricated working electrode was named as CoP/GCE. The electrochemical measurements were carried out using a three-electrode system, which employed a platinum wire as a counter electrode, Hg/HgO electrode as a reference, and 0.1M NaOH solution was used as electrolyte.

Calculation methods

The theoretical density functional theory (DFT) calculations are performed with CASTEP package. CASTEP is available as part of Materials Studio. Accelrys Inc., Suite 100 San Diego, CA 92121, USA. Generalized gradient approximation (GGA) with Perdew-Burke-Ernzerh (PBE) functional²¹ was used for exchange and correlation. The double numeric basis with polarization functions (DNP) was used as the atomic basis set. The tolerance of density convergence in self-consistent field (SCF) was set to 1×10^{-5} eV/atom. The energy tolerance was 5×10^{-5} eV/atom. The force tolerance was chosen as 0.1 eV/Å for full relaxation of the structure.

Results and discussion

The crystal structure of as-prepared samples was determined by XRD. Figure 1A (a) shows the XRD pattern of

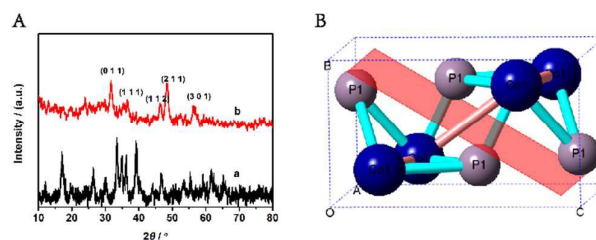


Figure 1. (A) The XRD patterns of cobalt precursor (I) and final product CoP (II); (B) Crystal structure of CoP.

the cobalt salt precursor whose peaks matched well with that of orthorhombic basic cobalt carbonate hydroxide $\text{Co}(\text{OH})_2(\text{CO})_2$ (JCPDS 48-0083). All of the diffraction peaks in Figure 1A (b) are from CoP (JCPDS 27-0497), which indicates that crystalline CoP was prepared after low-temperature phosphidation. As seen in Figure 1A (a), the main peaks of CoP appearing at 31.6° , 36.3° , 46.2° , 48.1° , and 56.8° correspond to the (011), (111), (112), (211), and (301) crystal faces of CoP, respectively. Figure 1B illustrates the molecular stick model of CoP, which is orthorhombic. In the monophosphide CoP, the metal atoms form triangular prisms, where the metal atoms surround the nonmetal atoms. Thus, Co has a greater chance to be exposed to the outside and permits more access to active corner and edge sites on the crystallite surfaces. The lattice plane of (011) is marked in Figure 1B.

The X-ray photoelectron spectroscopy (XPS) in the P (2p) and Co ($2p_{3/2}$) regions for CoP nanorods are shown in Figure 2. Two peaks are apparent in the Co ($2p_{3/2}$) region at 779.2 and 782.4 eV, along with two peaks in the P (2p) region at 129.9 and 134.6 eV; the peaks are close to the binding energies (BEs) of Co and P in CoP, respectively. The P (2p) binding energy of 129.9 eV is negatively shifted from that of elemental P (130.2 eV), and the Co (2p) BE of 779.2 eV is positively shifted from that of Co metal (778.1-778.2 eV). This suggests that the Co atom in CoP has a partial positive charge ($\text{Co}^{\delta+}$), while the P has a partial negative charge, implying the transfer of electron density from Co to P.^{22, 23} When compared with Co_3O_4 , the binding energy of the Co atom in CoP is lower than that in Co_3O_4 (779.58 eV).²⁴ The average positive charge of Co atom in CoP is below 3 ($0 < \delta < 3$).

The morphologies of the cobalt salt precursor and final product CoP (Figure 3C) were further investigated by FESEM and TEM. As displayed in Figures 3A and B, the precursor is constructed by nanorods. After low-temperature phosphidation, the obtained CoP kept the original morphology of its precursor, even though the nanorods became tougher. The TEM images in Figures 3D and E further reveal that the surface of CoP nanorods is rough and porous. The high resolution TEM (HRTEM) image (Figure 3E) of the CoP nanorods shows clear lattice fringes, which confirms single-crystallinity of the CoP. The lattice spacing is 0.28 nm between adjacent lattice planes in the image and corresponds to the distance between two (011) crystal planes. This loose and porous nanostructure is beneficial to the transfer of electrolytes and the adsorption of glucose on its surface. This makes it possible to obtain quick measurements of glucose in solution.

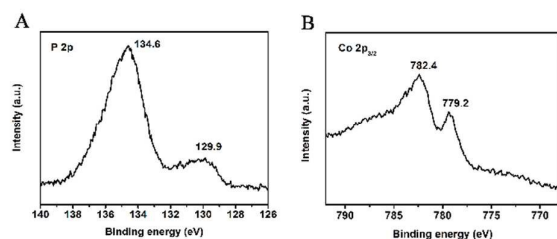


Figure 2. XPS spectra in the (A) P (2p) and (B) Co (2p) spectrum for CoP nanorods.

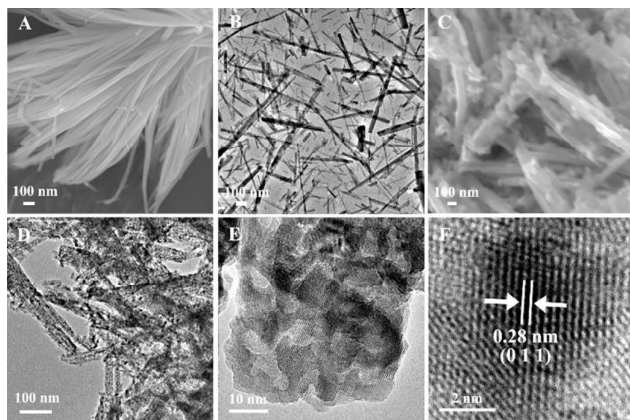


Figure 3. FESEM of CoP (C) and its precursor (A); TEM of precursor (B); TEM of CoP (D, E) and its high resolution (HRTEM) image (F).

Figure 4A shows the cyclic voltammograms (CVs) of the bare GCE and the CoP/GCE in 0.1 M NaOH solution at a scanning rate of 25 mV s⁻¹. It is clear that no redox peak is observed for the bare electrode (Figure 4A(a)), suggesting that it is electrochemically silent in the potential range. While a pair of obvious redox peaks can be seen at CoP/GCE, its redox peaks in N₂-saturated (Figure 4A(b)) and air-saturated (Figure 4A(c)) NaOH solution are very similar, which suggests that the CoP is not sensitive to oxygen. The two couples of peaks shown in Figure 4A are attributed to the redox reaction of CoP on the electrode surface in alkaline medium. The electrochemical reaction process of CoP in an alkaline electrolyte solution is still not very clear. However, according to XPS analysis, the valence state of the Co ion in CoP is below +3. The reaction properties of CoP are very similar to that of other Co₃O₄ reported in a previous study, which discovered two pairs of well-defined and symmetric redox peaks in an alkaline medium.²⁵ The reaction equations of this process are described as follows:

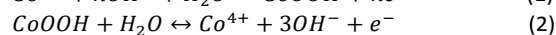


Figure 4B represents the CVs of CoP/GCE at different scanning rates (1~200 mVs). The anodic peak shows a slight positive shift, while the cathodic peak moves negatively with the increase of the scan rate, indicating a quasi-reversible electron transfer reaction for the electrochemical reactions

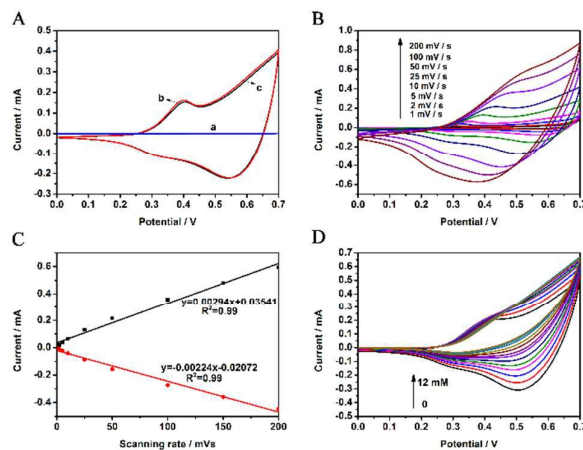
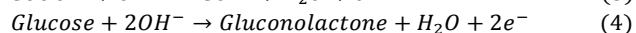
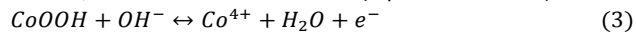


Figure 4. (A) CVs of (a) bare GCE modified by CoP in (b) N₂-saturated and (c) air-saturated NaOH solution (0.1 M) at a scanning rate of 25 mV s⁻¹. (B) CVs of CoP/GCE at different scanning rates. (C) The linear fitting of peak current from B. (D) CVs with addition of different amounts glucose in NaOH solution at a scanning rate of 25 mV s⁻¹.

in Equations 1 and 2. Moreover, a continuous increase in anodic and cathodic peak currents occurs as the scanning rate is increased. The peak current for both the oxidation and the reduction are proportional to the scan rate, as depicted in Figure 4C, implying that the electrochemical reaction on the surface of the CoP/GCE is a typical surface controlled process, which is ideal for electrochemical glucose sensing. Figure 4D shows the CV change with successive additions of glucose in the NaOH solution. After the addition of glucose in the test solution, the oxidation current of the test electrode increased, an indication that the reaction of glucose is catalyzed by the CoP-modified electrode.

Figure 5 displays the amperometric responses of 0.5 mM glucose on bare GCE and the CoP-modified electrode at different applied potentials. It is clear that no response was observed below 0.8 V on the bare electrode. Only when the applied potential was higher than 0.9 V, a weak response current appeared, which indicated that the oxidation reaction of glucose on the bare electrode is a sluggish kinetic process with a large energy barrier. However, at the surface of CoP-modified electrode, an obvious current response for 0.5 mM glucose was observed even at 0.3 V. With the increase of the test potential, the response current increased correspondingly. This suggests that CoP is a good electrochemical catalyst for the oxidation reaction of glucose. It is generally believed that nanomaterials act like an electron delivery system in the electrocatalytic process to accelerate the electron transfer and enhance the electrocatalytic ability of the biosensor. Further, the Co^{δ+} in CoP is easily self-oxidized to Co (III) in the electrochemical reaction process, and after the injection of glucose, the electrooxidation of glucose is mostly mediated by CoOOH/Co⁴⁺ in an alkaline solution (Equations 3 and 4).



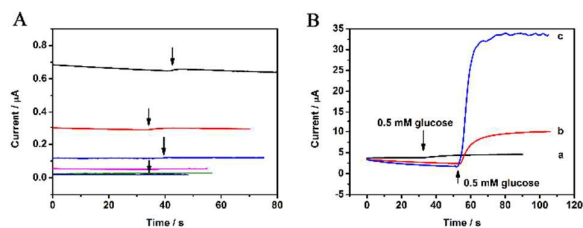
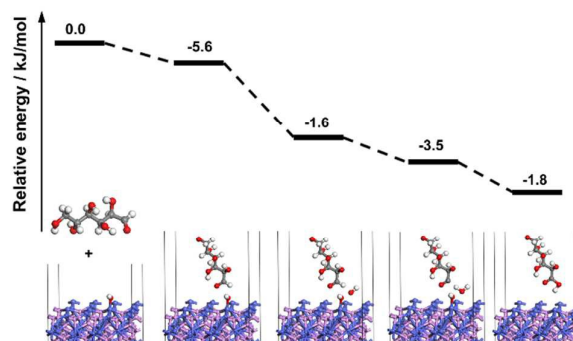


Figure 5. (A) Current responses of bare GCE for glucose at different applied potential of 0.5, 0.6, 0.7, 0.8, 0.9, and 1.0 V, respectively (down to up). (B) The amperometric response of CoP/GCE for glucose at applied potential of (a) 0.3 V, (b) 0.4 V, and (c) 0.5 V.

In order to better understand the electrocatalytic process of CoP to glucose, a theoretical study of the electrocatalytic process is carried out by density-functional theory (DFT) calculations. As observed from the XRD pattern and HRTEM of CoP in Figures 3 and 4, respectively, the (011) crystal face is the lowest-index face of CoP that was observed. The exposed low-index facet with well-defined geometric and electronic structures could be well-exploited as the active spots for various types of reactions with enhanced catalytic activity. In NaOH solution, glucose, H₂O, and OH⁻ are considered as three reactive species on the CoP surface in the glucose electrocatalytic reaction process. According to the following calculated reaction energy diagram (shown in Scheme 1), the reaction of glucose with OH⁻ is far easier than that of glucose with H₂O. Additionally, the adsorption energy of glucose on the CoP surface is stronger than that on the OH-covered CoP surface. In the NaOH solution, the surface of CoP would be negatively charged and easily covered by OH⁻. Hence, we proposed that the main electrocatalytic reaction was controlled by the adsorbed structure of glucose on the OH-covered CoP (011) surface. The calculated reaction energy diagram is shown in Scheme 1c. In the reaction system, a hydrogen bond formed between glucose and OH-covered CoP and another OH⁻ in the solution; the water molecule was formed by a proton transfer from the -CHO group of glucose to OH⁻ in the alkaline solution. The gluconic acid was produced by the transfer of OH⁻ from the CoP surface without any transition states.²⁶

The anti-interference performance towards other physiological species is one of the biggest concerns of the glucose electrochemical sensor. The test potential has a large influence on the anti-interference ability of the sensor. As shown in Figure 6, the response currents of 0.05 mM ascorbic acid (AA), dopamine (DA), and uric acid (UA) did not increase and were far lower than that of glucose, especially when a low potential of 0.3 V was applied. This suggests that these species had no obvious interference in the oxidation of glucose in our designed biosensor. However, the response of glucose also weakened at 0.3 V, which suggests that 0.4 V is a suitable potential for CoP/GCE to detect glucose.



Scheme 1. (a) The relative reaction energy diagram of glucose with OH⁻ and H₂O; (b) different adsorption modes of glucose on CoP; (c) reaction energy diagram of glucose oxidation reaction on OH-covered CoP (011) surface.

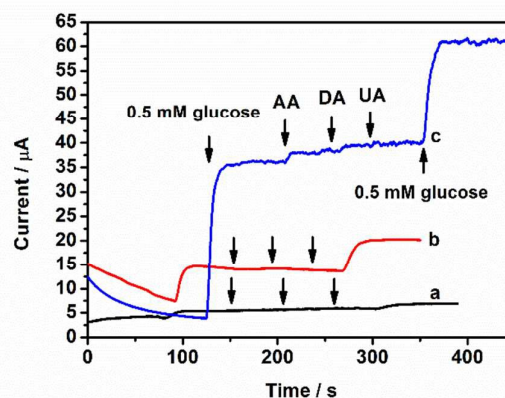


Figure 6. (A) The current responses of CoP/GCE for glucose and the interfering species (a) at 0.3 V, (b) 0.4 V, and (c) 0.5 V.

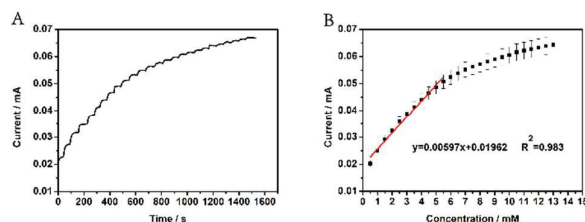


Figure 7. (A) The amperometric response of CoP/GCE for glucose at applied potential of 0.4 V. (B) The linear fitting of amperometric response.

After analyzing the electrocatalytic mechanism and feasibility of CoP for detecting glucose, the biosensing performance of the CoP-based biosensor was further evaluated. Figure 7A displays the amperometric responses of CoP/GCE for successive additions of 0.5 mM glucose to the electrolyte under stirring at an applied potential of 0.4 V. The calibration curves of response (Figure 7B) show a linear response with a correlation coefficient of 0.98, and the linear range increased to 5.5 mM. Simultaneously, the sensitivity was

about 116.8 $\mu\text{A}/(\text{cm}^2 \text{ mM})$, and the limit of detection was 9 μM .

Conclusions

In this work, cobalt phosphide was analyzed as a new biosensing material for the detection of glucose. TEM characterization suggests that the surface of CoP is rough and porous, which causes more crystal faces to be exposed in electrolyte solution and benefits the diffusion of glucose in the electrode material. In order to thoroughly understand the electrocatalytic reaction mechanism, electrochemical measurements and theoretical calculations were carried out in detail. In an alkaline solution, the reaction barrier from the direct adsorption of glucose on the electrode surface was relatively high. The first transition state for OH^- transfer from the electrode surface to the $-\text{CHO}$ group of glucose is a rate-determining step. The electrochemical results indicate that CoP nanorods can accelerate the electron transfer to glucose and significantly enhance the electrocatalytic ability of a biosensing electrode.

Acknowledgements

This work is financially supported by Fundamental Research Funds for the Central Universities (XDJK2015D030); National Natural Science Foundation of China (21163021, 21203154, 31200700, 21375108); Program for Excellent Talents in Chongqing (102060-20600218); Chongqing Key Laboratory for Advanced Materials and Technologies of Clean Energies; Computational resources have been provided by HPC of Faculty of Materials and Energy in Southwest University.

References

1. F. Gao, F. Luo, X. Chen, W. Yao, J. Yin, Z. Yao and L. Wang, *Talanta*, 2009, **80**, 202-206.
2. V. Scognamiglio, *Biosensors and Bioelectronics*, 2013, **47**, 12-25.
3. C. A. Marquette and L. c. J. Blum, *Analytica Chimica Acta*, 1999, **381**, 1-10.
4. H. V. Hsieh, Z. A. Pfeiffer, T. J. Amiss, D. B. Sherman and J. B. Pitner, *Biosensors and Bioelectronics*, 2004, **19**, 653-660.
5. J. Wang, *Chemical Reviews*, 2008, **108**, 814-825.
6. A. S. Kumar, P. Y. Chen, S. H. Chien and J. M. Zen, *Electroanalysis*, 2005, **17**, 210-222.
7. S. Park, H. Boo and T. D. Chung, *Analytica Chimica Acta*, 2006, **556**, 46-57.
8. A. Salimi and M. Roushani, *Electrochemistry Communications*, 2005, **7**, 879-887.
9. Y. Xian, Y. Hu, F. Liu, Y. Xian, H. Wang and L. Jin, *Biosensors and Bioelectronics*, 2006, **21**, 1996-2000.
10. J.-S. Ye, C.-W. Chen and C.-L. Lee, *Sensors and Actuators B: Chemical*, 2015, **208**, 569-574.
11. D. Zhai, B. Liu, Y. Shi, L. Pan, Y. Wang, W. Li, R. Zhang and G. Yu, *ACS Nano*, 2013, **7**, 3540-3546.

12. X. Kang, Z. Mai, X. Zou, P. Cai and J. Mo, *Analytical Biochemistry*, 2007, **363**, 143-150.
13. L.-C. Jiang and W.-D. Zhang, *Biosensors and Bioelectronics*, 2010, **25**, 1402-1407.
14. S. Ci, T. Huang, Z. Wen, S. Cui, S. Mao, D. A. Steeber and J. Chen, *Biosensors and Bioelectronics*, 2014, **54**, 251-257.
15. J. Wu, Q. Wang, A. Umar, S. Sun, Y. Gao, J. Wang, L. Huang and Z. Guo, *Sensor Letters*, 2014, **12**, 69-74.
16. J. Chen, W.-D. Zhang and J.-S. Ye, *Electrochemistry Communications*, 2008, **10**, 1268-1271.
17. Q. Liu, J. Tian, W. Cui, P. Jiang, N. Cheng, A. M. Asiri and X. Sun, *Angewandte Chemie-International Edition*, 2014, **53**, 6710-6714.
18. J. Tian, Q. Liu, A. M. Asiri and X. Sun, *Journal of the American Chemical Society*, 2014, **136**, 7587-7590.
19. Z. Pu, Q. Liu, P. Jiang, A. M. Asiri, A. Y. Obaid and X. Sun, *Chemistry of Materials*, 2014, **26**, 4326-4329.
20. P. Hohenberg and W. Kohn, *Physical review*, 1964, **136**, B864.
21. J. P. Perdew, K. Burke and M. Ernzerhof, *Physical review letters*, 1996, **77**, 3865.
22. P. Jiang, Q. Liu, C. Ge, W. Cui, Z. Pu, A. M. Asiri and X. Sun, *Journal of Materials Chemistry A*, 2014, **2**, 14634-14640.
23. Z. Huang, Z. Chen, Z. Chen, C. Lv, M. G. Humphrey and C. Zhang, *Nano Energy*, 2014, **9**, 373-382.
24. W. Hu, L. Wang, Q. Wu and H. Wu, *Advanced Powder Technology*, 2014, **25**, 1780-1785.
25. Y. Ding, Y. Wang, L. Su, M. Bellagamba, H. Zhang and Y. Lei, *Biosensors and Bioelectronics*, 2010, **26**, 542-548.
26. T. Ishimoto, H. Kazuno, T. Kishida and M. Koyama, *Solid State Ionics*, 2014, **262**, 328-331.